

Isochoric Heat Capacity for Toluene near Phase Transitions and the Critical Point[†]

Nikolai G. Polikhronidi,[‡] Ilmutdin M. Abdulagatov,^{*,‡,§} Joseph W. Magee,[§] and Rabiya G. Batyrova[‡]

Institute of Physics of the Dagestan Scientific Center of the Russian Academy of Sciences, 367005 Makhachkala, M. Yaragskogo Str.94, Dagestan, Russia, and Physical and Chemical Properties Division, National Institute of Standards and Technology, 325 Broadway, Boulder, Colorado 80305-3328

New measurements of isochoric heat capacity C_V for toluene near phase transitions and the critical point are presented. Measurements were made with a high-temperature, high-pressure, adiabatic calorimeter of nearly constant volume. The inner volume of the calorimeter is $(104.441 \pm 0.002) \text{ cm}^3$ at 297.15 K and 0.1 MPa. The heat capacity of the empty calorimeter C_0 was measured by use of a reference fluid (helium-4) with a well-known heat capacity (uncertainty of 0.1%). The temperature of the sample was measured with a 10Ω PRT with an uncertainty of 10 mK. Uncertainties of the heat capacity measurements are estimated to be 2% to 3%. Measurements were made in the single- and two-phase regions. The experimental values of phase transition temperatures $T_S(\rho)$ and single- and two-phase isochoric heat capacities (C_{V1} , C_{V2}) on each measured isochore were determined by use of a quasi-static thermogram method. Measurements were made along 12 isochores between $(199.3 \text{ and } 525.0) \text{ kg}\cdot\text{m}^{-3}$ in the temperature range from (411 to 620) K. The temperature dependence of single- (C_{V1}) and two-phase (C_{V2}) isochoric heat capacities along the coexistence curve and along near-critical isochores, the isochoric heat capacity jumps ΔC_V , and the density and temperature on the coexistence curve near the critical point are discussed. The values of the critical parameters (critical temperature, density, and pressure) of toluene were derived from the experimental measurements of density, temperature, and heat capacity at saturation in the immediate vicinity of the critical point. The scaling equations were used to express measured values of C_V and density along the coexistence curve. The results of the measurements are compared with values calculated from various equations of state. The data can be used to improve the equation of state and to develop a crossover equation in the critical region.

Introduction

Toluene is often used as a solvent, and reliable thermodynamic properties, including C_V , are of direct technological importance. In this paper we present accurate measurements of the isochoric heat capacity of toluene in the critical region. The measurements were obtained with a high-temperature, high-pressure adiabatic calorimeter of nearly constant volume. Toluene has been recommended as a reference standard for the transport (thermal conductivity and viscosity) properties of liquids (Nieto de Castro et al.¹). Toluene is also a suitable reference standard for thermodynamic properties and an important calibration standard. Previously, the thermodynamic properties (PVT , C_P , speed of sound, etc.) of toluene were measured in different laboratories with a variety of experimental techniques. This is the first study of the constant-volume heat capacity C_V of toluene.

Experimental Section

The experimental apparatus used in this paper is the same as was previously employed for the measurement of

light and heavy water.² Since the apparatus has been described in detail in our previous papers (Polikhronidi et al.,^{2–4} Abdulagatov et al.^{5,6}), only a brief discussion will be given here. The calorimeter is a multilayered system that consists of an internal thin-walled (0.8 mm to 1.0 mm thick) steel vessel, outer adiabatic shells, and a semiconductor layer (cuprous oxide) between them of 3.5 mm thickness. The outer adiabatic shell is made of the same steel but has walls 6 to 8 mm in thickness. The heat capacity of the empty calorimeter C_0 was determined experimentally using a reference substance (helium-4) with well-known (uncertainty of 0.1%) heat capacities.⁷ The measured values of C_0 range from 60 to 70 $\text{J}\cdot\text{K}^{-1}$.

The volume of the calorimetric vessel, $V_{297} = 104.441 \pm 0.002 \text{ cm}^3$ at 297.15 K and at 0.1 MPa, was determined by filling with pure water. The working volume of the calorimeter V_{PT} is a function of temperature and pressure with an uncertainty of 0.05%. C_V was measured by the continuous-heating method. The rate of temperature change was proportional to the power supplied to the internal heater and varied from $10^{-3} \text{ K}\cdot\text{s}^{-1}$ (far from the critical point) to $5 \times 10^{-5} \text{ K}\cdot\text{s}^{-1}$ (in the critical region). The heat capacity was obtained from the measurements of m (mass of the sample in the calorimeter), ΔQ (amount of electrical energy released by the internal heater), C_0 (heat capacity of the empty calorimeter), and ΔT (temperature rise resulting from addition of electrical energy ΔQ). The temperature was measured with a 10Ω standard platinum resistance

[†] This contribution will be part of a special print edition containing papers presented at the Fourteenth Symposium on Thermophysical Properties, Boulder, CO, June 25–30, 2000.

^{*} To whom correspondence should be addressed. E-mail: ilmutdin@boulder.nist.gov.

[‡] Institute of Physics of the Dagestan Scientific Center of the Russian Academy of Sciences.

[§] National Institute of Standards and Technology.

Table 1. Experimental Values of the Single- and Two-Phase Isochoric Heat Capacities of Toluene

| T | C_V |
|---|--|---|--|---|--|---|--|---|--|---|--|
| K | $\text{kJ}\cdot\text{kg}^{-1}\cdot\text{K}^{-1}$ |
| $\rho = 525.0 \text{ kg}\cdot\text{m}^{-3}$ | | $\rho = 413.4 \text{ kg}\cdot\text{m}^{-3}$ | | $\rho = 316.9 \text{ kg}\cdot\text{m}^{-3}$ | | $\rho = 299.5 \text{ kg}\cdot\text{m}^{-3}$ | | $\rho = 259.1 \text{ kg}\cdot\text{m}^{-3}$ | | $\rho = 217.5 \text{ kg}\cdot\text{m}^{-3}$ | |
| 411.28 | 2.695 ^a | 582.59 | 3.883 ^a | 571.20 | 3.735 ^a | 570.84 | 3.780 ^a | 590.61 | 4.826 ^a | 587.08 | 4.806 ^a |
| 422.20 | 2.826 ^a | 582.87 | 3.905 ^a | 571.49 | 3.743 ^a | 570.90 | 3.792 ^a | 590.82 | 4.875 ^a | 587.36 | 4.831 ^a |
| 422.91 | 2.824 ^a | 583.15 | 3.891 ^a | 571.77 | 3.764 ^a | 570.99 | 3.794 ^a | 591.04 | 4.836 ^a | 587.72 | 4.920 ^a |
| 433.83 | 2.816 ^a | 586.08 | 3.960 ^a | 584.52 | 4.161 ^a | 571.22 | 3.810 ^a | 591.21 | 4.943 ^a | 588.94 | 4.932 ^a |
| 453.91 | 2.909 ^a | 586.96 | 4.038 ^a | 584.81 | 4.185 ^a | 588.14 | 4.466 ^a | 592.98 | 5.357 ^a | 589.19 | 4.987 ^a |
| 475.08 | 3.012 ^a | 587.42 | 4.118 ^a | 590.94 | 4.610 ^a | 588.23 | 4.471 ^a | 593.24 | 5.462 ^a | 590.20 | 5.084 ^a |
| 497.72 | 3.105 ^a | 587.93 | 4.081 ^a | 591.21 | 4.602 ^a | 592.52 | 4.950 ^a | 593.41 | 5.572 ^a | 590.76 | 5.133 ^a |
| 515.04 | 3.145 ^a | 588.25 | 4.110 ^a | 591.58 | 4.634 ^a | 592.64 | 5.011 ^a | 593.53 | 5.743 ^a | 591.08 | 5.148 ^a |
| 534.64 | 3.236 ^a | 588.35 | 4.130 ^a | 592.98 | 4.931 ^a | 592.75 | 5.026 ^a | 593.49 | 5.664 ^a | 591.22 | 5.221 ^a |
| 544.52 | 3.203 ^a | 588.35 | 3.181 | 593.35 | 5.180 ^a | 592.89 | 5.050 ^a | 593.65 | 5.874 ^a | 591.51 | 5.260 ^a |
| 544.46 | 3.290 ^a | 588.40 | 3.140 | 593.64 | 5.354 ^a | 593.65 | 5.506 ^a | 593.65 | 4.638 | 591.63 | 5.270 ^a |
| 555.55 | 3.287 ^a | 588.55 | 3.106 | 593.77 | 5.535 ^a | 593.81 | 5.912 ^a | 593.72 | 4.550 | 591.63 | 3.916 |
| 558.50 | 3.301 ^a | 588.62 | 3.100 | 593.83 | 5.740 ^a | 593.85 | 6.420 ^a | 593.81 | 4.461 | 591.89 | 3.813 |
| 562.12 | 3.330 ^a | | $\rho = 369.9 \text{ kg}\cdot\text{m}^{-3}$ | 593.85 | 5.847 ^a | 593.87 | 6.915 ^a | 593.90 | 4.270 | 592.32 | 3.735 |
| 562.12 | 2.640 | 586.60 | 4.091 ^a | 593.85 | 4.309 | 593.88 | 7.530 ^a | 594.55 | 3.530 | 592.54 | 3.664 |
| 562.74 | 2.614 | 586.97 | 4.080 ^a | 593.88 | 3.862 | 593.88 | 5.320 | 594.82 | 3.504 | 592.91 | 3.572 |
| 562.93 | 2.638 | 587.34 | 4.122 ^a | 594.16 | 3.781 | 593.96 | 4.722 | | $\rho = 238.6 \text{ kg}\cdot\text{m}^{-3}$ | 594.23 | 3.326 |
| 563.12 | 2.627 | 589.52 | 4.341 ^a | 594.36 | 3.540 | 594.00 | 4.195 | 584.01 | 4.547 ^a | 594.73 | 3.242 |
| 568.26 | 2.530 | 590.16 | 4.372 ^a | 594.92 | 3.430 | 594.13 | 3.864 | 584.19 | 4.512 ^a | 596.38 | 3.045 |
| 568.44 | 2.517 | 591.50 | 4.494 ^a | 597.25 | 3.135 | 594.14 | 3.698 | 584.60 | 4.571 ^a | 596.59 | 2.998 |
| 568.63 | 2.509 | 591.87 | 4.516 ^a | 597.51 | 3.108 | 594.46 | 3.620 | 584.78 | 4.533 ^a | 602.90 | 2.725 |
| 571.27 | 2.453 | 592.01 | 4.535 ^a | 601.07 | 2.905 | 594.74 | 3.540 | 589.26 | 4.861 ^a | 603.17 | 2.699 |
| 571.65 | 2.465 | 592.23 | 4.593 ^a | 601.26 | 2.920 | 595.28 | 3.512 | 589.65 | 4.894 ^a | 603.45 | 2.712 |
| 572.02 | 2.449 | 592.42 | 4.603 ^a | 601.44 | 2.897 | 605.74 | 2.923 | 591.57 | 5.086 ^a | 614.12 | 2.554 |
| 583.79 | 2.341 | 592.42 | 3.499 | | $\rho = 303.9 \text{ kg}\cdot\text{m}^{-3}$ | 605.92 | 2.950 | 591.97 | 5.205 ^a | 614.48 | 2.569 |
| 584.07 | 2.308 | 592.70 | 3.384 | 555.60 | 3.540 ^a | 606.65 | 2.914 | 592.70 | 5.234 ^a | 614.85 | 2.537 |
| 584.35 | 2.359 | 592.79 | 3.339 | 555.81 | 3.576 ^a | 620.11 | 3.017 | 592.79 | 5.390 ^a | | $\rho = 199.3 \text{ kg}\cdot\text{m}^{-3}$ |
| | | 592.93 | 3.321 | 556.05 | 3.503 ^a | | $\rho = 282.1 \text{ kg}\cdot\text{m}^{-3}$ | 592.87 | 5.435 ^a | 582.04 | 4.612 ^a |
| 576.94 | 3.680 ^a | 593.13 | 3.300 | 560.58 | 3.575 ^a | 585.87 | 4.402 ^a | 592.93 | 5.412 ^a | 582.21 | 4.602 ^a |
| 577.55 | 3.701 ^a | 593.53 | 3.207 | 560.76 | 3.592 ^a | 586.30 | 4.445 ^a | 592.96 | 5.482 ^a | 582.51 | 4.641 ^a |
| 578.20 | 3.724 ^a | 596.29 | 2.907 | 561.15 | 3.586 ^a | 586.67 | 4.433 ^a | 592.96 | 4.282 | 582.82 | 4.665 ^a |
| 579.13 | 3.737 ^a | 596.66 | 2.890 | 573.39 | 3.792 ^a | 587.02 | 4.480 ^a | 593.07 | 4.258 | 584.17 | 4.791 ^a |
| 581.00 | 3.825 ^a | 597.03 | 2.762 | 573.46 | 3.809 ^a | 588.97 | 4.560 ^a | 593.16 | 4.143 | 584.38 | 4.820 ^a |
| 581.16 | 3.795 ^a | 602.54 | 2.701 | 591.69 | 4.754 ^a | 589.25 | 4.624 ^a | 593.25 | 4.043 | 584.60 | 4.813 ^a |
| 581.65 | 3.822 ^a | 602.72 | 2.689 | 591.92 | 4.767 ^a | 592.96 | 5.180 ^a | 593.55 | 3.929 | 585.94 | 4.824 ^a |
| 582.49 | 3.804 ^a | 602.90 | 2.673 | 593.35 | 5.347 ^a | 593.07 | 5.350 ^a | 594.62 | 3.612 | 586.28 | 4.902 ^a |
| 582.74 | 3.818 ^a | | | 593.67 | 5.543 ^a | 593.63 | 5.504 ^a | 598.33 | 3.165 | 586.87 | 4.890 ^a |
| 582.78 | 3.842 ^a | | | 593.86 | 6.287 ^a | 593.66 | 5.804 ^a | 598.74 | 3.132 | 587.52 | 4.974 ^a |
| 582.78 | 2.970 | | | 593.88 | 6.679 ^a | 593.81 | 6.603 ^a | 602.35 | 3.028 | 587.89 | 4.954 ^a |
| 582.79 | 2.967 | | | 593.88 | 4.820 | 593.83 | 6.974 ^a | 603.09 | 3.064 | 588.35 | 5.080 ^a |
| 582.83 | 2.884 | | | 593.90 | 4.620 | 593.87 | 7.353 ^a | | | 588.98 | 5.106 ^a |
| 582.95 | 2.868 | | | 594.09 | 3.692 | 593.87 | 5.676 | | | 589.09 | 5.076 ^a |
| 583.05 | 2.850 | | | 594.46 | 3.582 | 593.96 | 4.673 | | | 589.46 | 5.142 ^a |
| 586.01 | 2.697 | | | 594.78 | 3.519 | 593.99 | 4.325 | | | 589.68 | 5.196 ^a |
| 586.38 | 2.681 | | | 595.10 | 3.447 | 594.18 | 3.859 | | | 589.77 | 5.220 ^a |
| 586.75 | 2.674 | | | 602.63 | 2.914 | 594.64 | 3.642 | | | 589.77 | 3.630 |
| 590.92 | 2.640 | | | 602.82 | 2.923 | 601.99 | 3.205 | | | 590.61 | 3.476 |
| 591.29 | 2.617 | | | 603.00 | 2.897 | 602.27 | 3.196 | | | 591.89 | 3.274 |
| 591.66 | 2.651 | | | 612.31 | 2.830 | 602.54 | 3.180 | | | 592.99 | 3.110 |
| | | | | 612.49 | 2.811 | 611.12 | 3.154 | | | 595.65 | 2.830 |
| | | | | 612.67 | 2.823 | 611.49 | 3.208 | | | 597.50 | 2.727 |
| | | | | | | 611.85 | 3.143 | | | 600.45 | 2.602 |
| | | | | | | | | | | 601.82 | 2.596 |

^a Two-phase experimental point.

thermometer. The uncertainty of temperature measurements was less than 10 mK. The mass of the sample was determined by direct weighing. The density of the sample was calculated as the ratio of the mass of the sample m to the working volume V_{PT} of the calorimetric vessel, $\rho = m/V_{PT}$. The uncertainty in density measurements is about 0.1%. The correction related to the nonisochoric behavior during heating was calculated with an uncertainty of 4.0%. The absolute uncertainty in C_V due to a brief excursion of the adiabatic control is about $13 \text{ J}\cdot\text{K}^{-1}$. Surface-temperature gradients were measured with differential copper-constantan thermocouples. The temperature gradients on the surface of the calorimeter vessel were minimized by shield control to within $0.02 \text{ K}\cdot\text{m}^{-1}$. On the basis of a detailed analysis of all sources of uncertainties likely to

affect the determination of C_V with the present system, the combined standard uncertainty of measuring heat capacity, with an allowance for the propagation of the uncertainty related to the nonisochoric conditions of the process, was 2 to 3%. The toluene sample was free of water and dissolved air and had a purity of 0.9982 mole fraction, with principal impurities being benzene and thiophene.

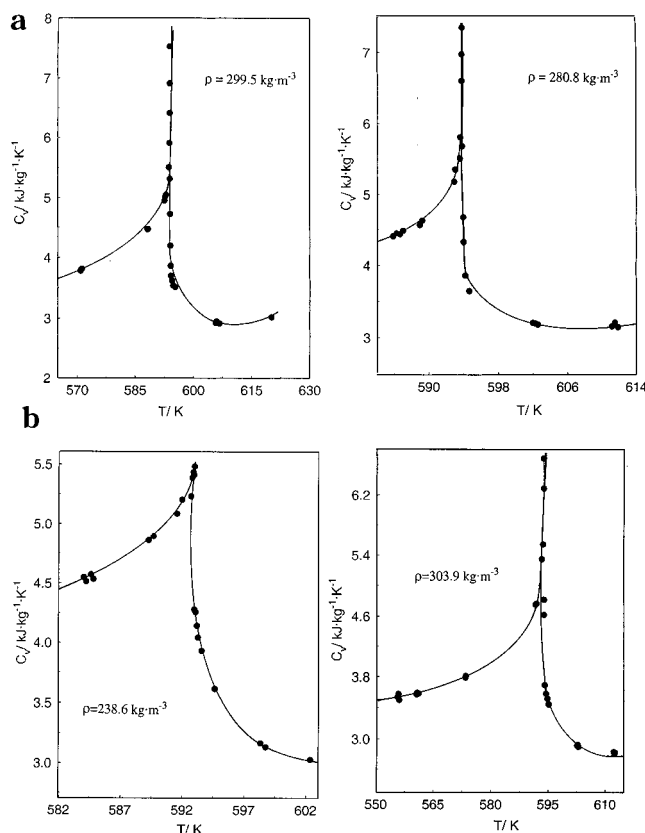
Results and Discussion

The measured single- and two-phase isochoric heat capacities C_V for toluene as a function of temperature along various isochores are presented in Table 1. Single- (C_{V1}) and two-phase (C_{V2}) isochoric heat capacities, at saturation, for vapor and liquid densities are given in Table 2 together with values of saturated liquid and vapor densities (ρ'_s, ρ''_s)

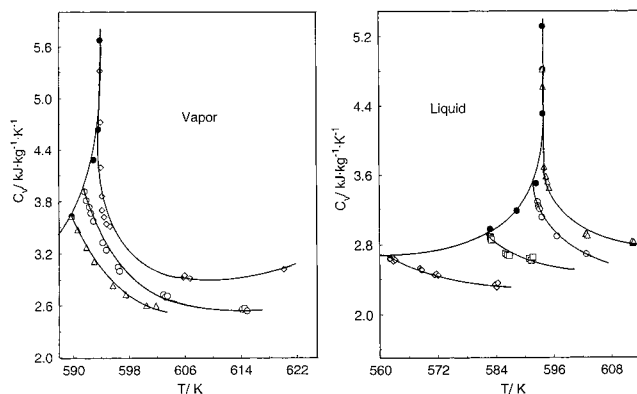
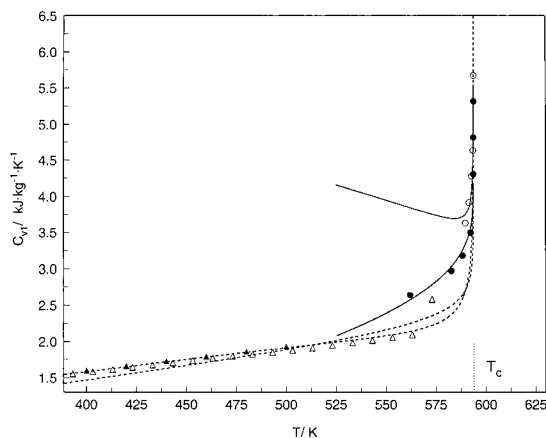
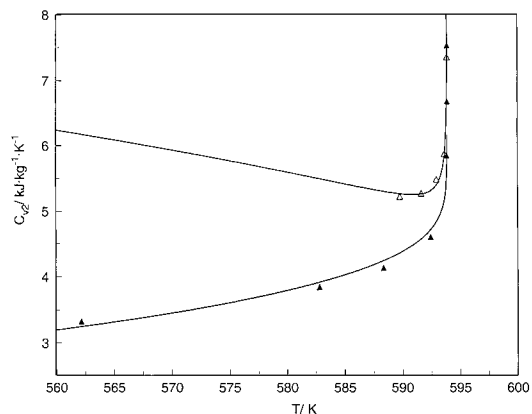
Table 2. Experimental Values of the Isochoric Heat Capacities, Densities, and Temperatures of Toluene along the Saturation Boundary

| T_s | ρ'_s | C'_{V2} | C'_{V1} | $\Delta C'_V$ |
|---------|-------------------------------|--|--|--|
| K | $\text{kg}\cdot\text{m}^{-3}$ | $\text{kJ}\cdot\text{kg}^{-1}\cdot\text{K}^{-1}$ | $\text{kJ}\cdot\text{kg}^{-1}\cdot\text{K}^{-1}$ | $\text{kJ}\cdot\text{kg}^{-1}\cdot\text{K}^{-1}$ |
| 562.122 | 525.0 | 3.330 | 2.640 | 0.690 |
| 582.785 | 451.3 | 3.842 | 2.973 | 0.869 |
| 588.347 | 413.4 | 4.130 | 3.181 | 0.949 |
| 592.423 | 369.9 | 4.603 | 3.499 | 1.104 |
| 593.847 | 316.9 | 5.847 | 4.309 | 1.538 |
| 593.882 | 303.9 | 6.679 | 4.820 | 2.859 |
| 593.884 | 299.5 | 7.530 | 5.320 | 2.210 |

| T_s | ρ''_s | C''_{V2} | C''_{V1} | $\Delta C''_V$ |
|---------|-------------------------------|--|--|--|
| K | $\text{kg}\cdot\text{m}^{-3}$ | $\text{kJ}\cdot\text{kg}^{-1}\cdot\text{K}^{-1}$ | $\text{kJ}\cdot\text{kg}^{-1}\cdot\text{K}^{-1}$ | $\text{kJ}\cdot\text{kg}^{-1}\cdot\text{K}^{-1}$ |
| 593.865 | 282.1 | 7.353 | 5.676 | 1.677 |
| 593.647 | 259.1 | 5.874 | 4.638 | 1.236 |
| 592.959 | 238.6 | 5.482 | 4.282 | 1.200 |
| 591.626 | 217.5 | 5.270 | 3.916 | 1.354 |
| 589.775 | 199.3 | 5.220 | 3.630 | 1.590 |

**Figure 1.** (a and b) Measured single- and two-phase isochoric heat capacities of toluene as a function of temperature near the phase transition points in the critical region; the solid curves are guides for the eye.

and temperatures (T_s). Measurements were made along 12 isochores (5 vapor and 7 liquid isochores), with densities of 199.3, 217.5, 238.6, 259.1, 282.1, 299.5, 303.9, 316.9, 369.9, 413.4, 451.3, and 525.0 $\text{kg}\cdot\text{m}^{-3}$. The measured temperature range was between 411 and 620 K. Very closely spaced measurements were made in the immediate vicinity of the coexistence curve in order to accurately determine the phase transition temperatures $T_s(\rho)$ for each measured isochore close to the critical density. Figures 1 and 2 show the measured isochoric heat capacity as a function of temperature for selected liquid and vapor near-critical densities. Figures 3 and 4 show the single- and two-phase liquid and vapor isochoric heat capacities at satu-

**Figure 2.** Measured single-phase isochoric heat capacities of toluene as a function of temperature near the phase transition curve along various liquid and vapor isochores; the solid curves are guides for the eye. Vapor: ●, values of C_V at saturation; ◇, 238.6 $\text{kg}\cdot\text{m}^{-3}$; ○, 217.5 $\text{kg}\cdot\text{m}^{-3}$; △, 199.3 $\text{kg}\cdot\text{m}^{-3}$. Liquid: ◇, 525.0 $\text{kg}\cdot\text{m}^{-3}$; □, 451.3 $\text{kg}\cdot\text{m}^{-3}$; ○, 369.9 $\text{kg}\cdot\text{m}^{-3}$; △, 303.9 $\text{kg}\cdot\text{m}^{-3}$.**Figure 3.** Single-phase liquid and vapor isochoric heat capacities of toluene along the coexistence curve together with values derived from speed of sound measurements (△, Zotov et al.;⁹ ▲, Okhotin et al.¹⁰) and values calculated from the (---) Goodwin⁸ EOS (○, C'_{V1} this work; ●, C_{V1} this work); the solid curves were calculated from the scaling relation, eq 2.**Figure 4.** Two-phase liquid and vapor isochoric heat capacities of toluene along the coexistence curve near the critical point: △, C'_{V12} this work; ▲, C_{V12} this work. The solid curves were calculated from the scaling relation, eq 2.

ration near the critical point together with values calculated from the nonanalytical equation of state (EOS) of Goodwin.⁸ The deviations between the present one-phase C_{V1} measurements and the values calculated from the Goodwin⁸ EOS along the coexistence curve in the critical region are

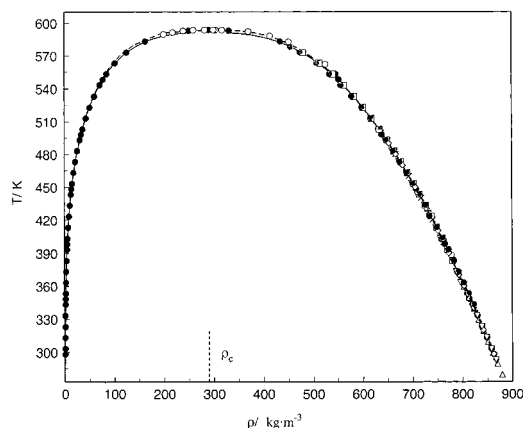


Figure 5. Liquid and vapor saturated densities of toluene from different authors together with calculated values from the (---) Goodwin⁸ and (—) Lemmon and Jacobsen¹¹ EOSs: ○, this work; ×, Okhotin et al.;¹⁰ ●, Mamedov and Akhundov;¹² △, Magee and Bruno;¹³ ▲, Francis;¹⁴ †, Chirico and Steele;¹⁵ □, Zotov et al.;¹⁶ ◇, Hales and Townsend;¹⁷ +, Shraiber and Pachenuk;¹⁸ ▽, Rudenko et al.¹⁹

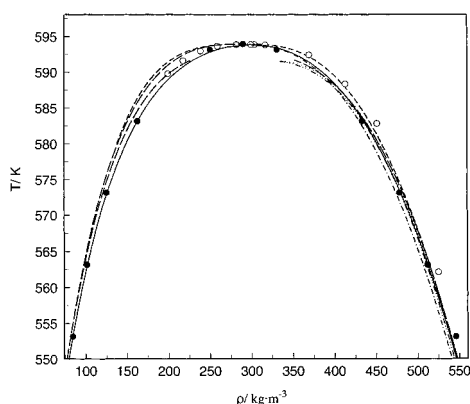


Figure 6. Liquid and vapor saturated densities of toluene together with values calculated from various equations in the asymptotical critical region: (---) Goodwin;⁸ (—) Lemmon and Jacobsen¹¹ EOS; ○, this work; ●, Mamedov and Akhundov;¹² (- · -) Francis;¹⁴ (· · ·) Hales and Townsend;¹⁷ (—) Simon;²⁰ (- · · ·) Riedel.²¹

about 20% for liquid isochores and 35% for vapor isochores. Figures 5 and 6 show the relation between saturated density and temperature derived in present calorimetric experiments, together with values reported by other authors. As Figure 6 shows, there is satisfactory agreement within 2% between the present data and the data reported by Mamedov and Akhundov.¹² In the temperature range far from the critical point ($T \leq 588$ K), the present results for the saturated liquid densities show good agreement to within about $\pm 1\%$ with the following experimental data: Zotov et al.;⁹ Okhotin et al.;¹⁰ Mamedov and Akhundov;¹² Magee and Bruno;¹³ Chirico and Steele;¹⁵ Hales and Townsend;¹⁷ Shraiber and Pechenyuk;¹⁸ and Rudenko et al.¹⁹ At high densities and at temperatures below 525 K, the agreement between the published data and the present results is very good (absolute average deviation = 0.3%). All of the data in this region show very good consistency. On the other hand, near the critical point, the saturated liquid data of Mamedov and Akhundov deviate by 2% from the present results, while the saturated vapor densities deviate by about 3%. While the underlying measurements of Mamedov and Akhundov are believed to be very reliable, the extrapolation procedure used to calculate the saturation densities is prone to systematic errors near the critical

Table 3. Reported Values of the Critical Properties of Toluene

| T_c | P_c | ρ_c | ref |
|---------------------|---------------------|-------------------------------|-----------|
| K | MPa | $\text{kg}\cdot\text{m}^{-3}$ | |
| 593.88 ± 0.02 | 4.225 ± 0.008 | 296.9 ± 5 | this work |
| 593.95 | 4.2358 | 289.77 ± 2 | 12 |
| 592.20 | | | 16 |
| 591.80 | 4.1087 | | 22, 23 |
| 591.79 | 4.1040 | | 24 |
| 591.72 | | | 25 |
| 593.95 | | | 14 |
| 593.05 | | 291.3 | 20 |
| 591.75 ± 0.15^a | 4.1080 ± 0.01^a | 291.0 ± 5^a | 26 |
| 592.50 ± 1 | 4.1620 ± 0.05^a | 291.0 ± 3^a | 15 |
| 592.00 | | | 27 |
| 593.95 | 4.1600 | 290.0 | 28 |
| 593.95 ^c | 4.2365 ^a | 291.4 ± 1.2^a | 8 |
| 591.79 ^b | 4.1040 ^b | | 29 |
| 591.72 ^a | 4.1087 ^a | 292.0 ± 0.004^a | 30 |
| 593.95 | | | 31 |
| 593.95 | | | 32 |
| 591.95 | | | 33 |
| 591.80 ^d | | 291.4 ± 1.2^a | 17 |
| | | 291.3 ^a | |
| 591.5 ± 0.6 | 4.1070 ± 0.020 | | 34, 35 |
| 591.5 ± 0.1 | | | |
| 593.75 | 4.2150 | | 36 |
| 591.48 | 4.1086 | | 37 |
| 591.90 ± 0.05 | 4.111 ± 0.007 | 289.73 ± 0.92 | 38 |
| 591.79 ± 0.05 | 4.109 ± 0.007 | 291.56 ± 0.92 | |
| 591.75 ± 0.05 | 4.108 ± 0.007 | 291.56 ± 0.92 | |
| 593.75 | 4.2150 | | 39 |

^a Evaluated. ^b From ref 24. ^c From ref 12. ^d From refs 22 and 23.

point. The values of the saturated liquid densities calculated from the Goodwin EOS deviate from the present results by 2 to 3% in the immediate vicinity ($T_c \pm 1$ K) of the critical point. At temperatures below 592 K, the deviations are about 1.5% while, for vapor isochores in the immediate vicinity of the critical point ($T_c \pm 2$ K), the deviations of densities calculated from the Goodwin EOS are between 5% and 7%. The reason for this is that Goodwin fitted saturated vapor densities calculated from the thermodynamic relation (Clapeyron equation)

$$\frac{1}{\rho''_s} = \frac{1}{\rho'_s} + \frac{\Delta H_{\text{vap}}}{T} \frac{dP_s}{dT} \quad (1)$$

by using experimental saturated liquid densities ρ'_s , vapor pressures $P_s(T)$, and enthalpies of vaporization ΔH_{vap} . Due to propagated uncertainties, values derived from eq 1 are prone to systematic errors. Direct measurements of saturated vapor densities were not available to Goodwin.

From our experimental data on the coexistence curve, we have deduced values of the critical parameters (critical temperature, density, and pressure). The available literature data on the critical constants of toluene are given in Table 3. Our results for the critical temperature $T_c = 593.88 \pm 0.02$ K and critical density $\rho_c = 296.9 \pm 5$ $\text{kg}\cdot\text{m}^{-3}$ are in good agreement ($\Delta T_c = +0.07$ K, critical density is about +2.4%) with the values reported by other authors.^{12,20,28,31,32,36} However, the maximum deviation between the present critical temperature and the data recommended by other authors^{22-26,29,30,33} was -2.16 K, and the critical density differs by 3.3%. The published values of T_c , ρ_c , and P_c reported for toluene differ at the most by about 2.23 K, 8.5 $\text{kg}\cdot\text{m}^{-3}$, and 0.132 MPa, respectively. The data given in Table 3 were obtained by a variety of experimental methods

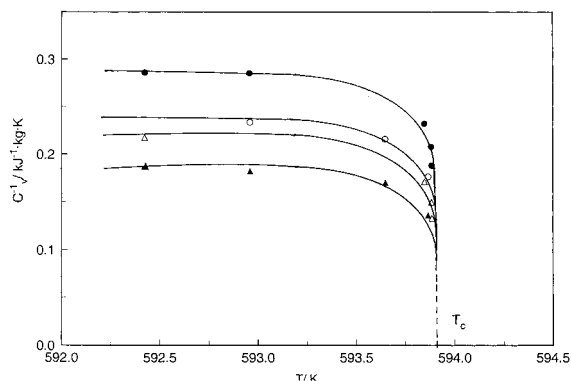


Figure 7. Measured single- and two-phase isochoric heat capacity C_V^{-1} for liquid and vapor isochores along the coexistence curve as a function of temperature: \circ , single-phase for vapor isochores; \bullet , single-phase for liquid isochores; \triangle , two-phase for liquid isochores; \blacktriangle , two-phase for vapor isochores. The solid curves are guides for the eye.

and calculation procedures. The critical properties for toluene were reviewed recently by Tsouopoulos and Amrose.²⁶ Detailed analyses of the critical properties of toluene are also reported in previous reviews by Kobe and Lynn²⁸ and Kudchadker et al.³⁰ The method of quasi-static thermograms²⁻⁶ was used in this work to measure the saturation temperatures and densities near the critical point. The uncertainties of this method are as follows: critical temperature, ± 0.02 K; critical density, $\pm 0.15\%$. This is an accurate method to measure the critical properties of fluids and has some distinct advantages compared with conventional methods. For more details of the method, see ref 2.

The experimental method most widely used to measure the coexistence curve is by directly observing the appearance and disappearance of the meniscus, but the observations are impeded by the development of critical opalescence. Moreover, as the critical point is approached, the difference between the liquid and vapor phases vanishes, and the visual determination of the moment at which the phase transition occurs becomes even less reliable. Therefore, the region of temperatures within $T_c \pm 1$ K becomes impractical for precise measurements with this method. The method of quasi-static thermograms makes it possible to obtain reliable data at temperatures in a region very close (± 0.01 K) to T_c .

The critical temperature and critical density for toluene were estimated from the present measurements on approach to zero of the inverse isochoric heat capacity at the critical point, where $C_V^{-1} = 0$. This corresponds to the divergence of C_V as the critical point is approached along the coexistence curve ($C_V^{-1} \approx t^\alpha$ or $C_V^{-1} \approx \Delta\rho^{\alpha/\beta}$). This criterion was used to determine the critical temperature and the critical density. Figures 7 and 8 show vapor and liquid single- and two-phase C_V^{-1} as a function of temperature and density along the coexistence curve in the immediate vicinity of the critical point. All of these curves extrapolate to zero, $C_V^{-1} \rightarrow 0$, at approximately the same temperature ($T_c = 593.88 \pm 0.02$ K) and the same density ($\rho_c = 293.8 \pm 5$ kg·m⁻³).

The critical behavior of the single- and two-phase isochoric heat capacities near the critical point along the coexistence curve and along the critical isochore can be expressed as in the scaling relation⁴⁰

$$C_V = A_0 t^{-\alpha} + A_1 t^{-\alpha+\Delta} + A_2 \quad (2)$$

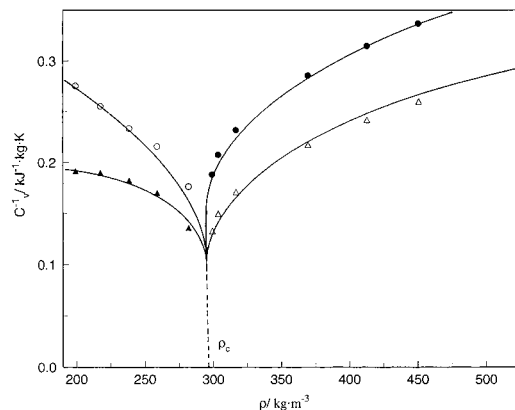


Figure 8. Single- and two-phase isochoric heat capacity C_V^{-1} for liquid and vapor isochores along the coexistence curve as a function of density: \circ , single-phase for vapor isochores; \bullet , single-phase for liquid isochores; \triangle , two-phase for liquid isochores; \blacktriangle , two-phase for vapor isochores. The solid curves are guides for the eye.

where $t = (T/T_c - 1)$, $\alpha = 0.112$ is the universal critical exponent,⁴¹ and $\Delta = 0.52$ is Wegner's leading correction-to-scaling critical exponent.⁴² The values of the fitted parameters A_i ($i = 0, 2$) derived from our measured values of C_V are given in Table 4 with their standard deviations. The values of the amplitude ratio of asymptotic terms $A^+_0/A^-_0 = 0.536 \pm 0.005$ for the isochoric heat capacity along the critical isochore in the temperature ranges $T > T_c$ (single-phase) and $T < T_c$ (two-phase) agree with values predicted by theoretical models (Ising model⁴³ $A^+_0/A^-_0 = 0.523$; field theory⁴⁴ $A^+_0/A^-_0 = 0.541$; and ϵ -expansion⁴⁴ $A^+_0/A^-_0 = 0.520$).

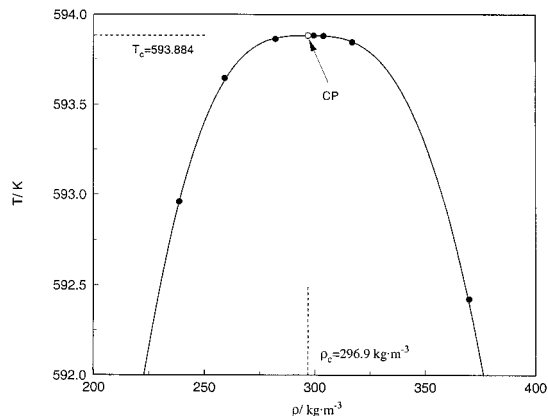
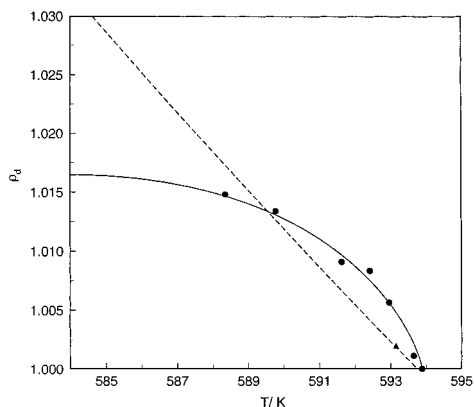
Figure 9 shows saturated temperature and density data from the present experiments in the critical region. Each derived saturated temperature in this figure has an uncertainty of ± 0.02 K, and the uncertainty in saturated density is about ± 0.3 kg·m⁻³, or 0.1%. For the two near-critical isochores (liquid, 303.9 kg·m⁻³; vapor, 282.1 kg·m⁻³), the temperature difference between phase transition points is only 0.017 K. Therefore, the critical temperature would be expected to be just slightly higher than $T_S = 593.86 \pm 0.02$ K and correspond to the critical density, which would be located between the densities 303.9 and 282.1 kg·m⁻³. The vapor–liquid critical temperature can be identified by the highest temperature on a pure fluid's phase boundary. The exact critical density is difficult to determine because of the size of the experimental temperature interval and the relatively small $dT_S/d\rho$ in the critical region. Therefore, the critical density can be determined only with less accuracy than the critical temperature. The scaling expression for density along the coexistence curve is⁴⁵

$$\Delta\rho = \pm B_0 t^\beta \pm B_1 t^{\beta+\Delta} + B_2 t^{1-\alpha} - B_3 t \quad (3)$$

where $\Delta\rho = (\rho/\rho_c - 1)$, $B_0 = 1.592 \pm 0.019$ is the asymptotic critical amplitude, $B_1 = 1.701 \pm 0.277$ is the nonasymptotic critical amplitude, $B_2 = 5.443 \pm 0.964$ is the singular diameter amplitude, $B_3 = 7.622 \pm 1.600$ is the rectilinear diameter amplitude, and $\beta = 0.325$ is the universal critical exponent.⁴¹ The value of critical density was derived by fitting measured saturated densities near the critical point. The value of the critical density was treated as a freely adjustable parameter. The nonlinear fit yielded a critical density of $\rho_c = 296.9 \pm 5$ kg·m⁻³. Figure 9 shows the shape of the coexistence curve near the critical point calculated from eq 3 together with measured values. It is evident from

Table 4. Parameters A_j for Eq 2

| A_0 | A_1 | A_2 | χ^2 | thermodynamic path |
|-------------------|---------------------|-------------------|----------|---|
| 0.3451 ± 0.05 | -3.5733 ± 0.71 | 3.2068 ± 0.23 | 0.98 | single-phase liquid C_{V1} along the coexistence curve |
| 0.5702 ± 0.09 | -5.0619 ± 1.15 | 4.0317 ± 0.38 | 0.75 | two-phase liquid C_{V2} along the coexistence curve |
| 1.8292 ± 0.06 | 4.2771 ± 1.37 | 0 | 1.12 | single-phase vapor C'_{V1} along the coexistence curve |
| 2.2790 ± 0.02 | 9.7796 ± 0.46 | 0 | 1.18 | two-phase vapor C'_{V2} along the coexistence curve |
| 0.0649 ± 0.03 | -14.1506 ± 3.90 | 4.4153 ± 0.27 | 1.65 | single-phase C_{V1} along the critical isochore ($T > T_c$) |
| 0.1212 ± 0.03 | -12.0104 ± 1.88 | 5.9150 ± 0.23 | 0.87 | two-phase C_{V2} along the critical isochore ($T < T_c$) |

**Figure 9.** Liquid and vapor saturated densities for toluene in the immediate vicinity of the critical point: ●, this work from C_V measurements; ○, derived critical point; the solid line represents the values of saturated density calculated from eq 3.**Figure 10.** Singular diameter as a function of temperature in the critical region for toluene: ●, this work from C_V measurements; the solid line represents the values of singular diameter calculated from eq 4; the dashed line represents the values of singular diameter calculated from the Simon²⁰ equation.

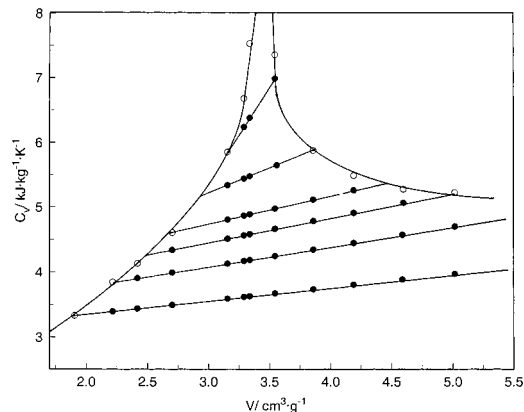
eq 3 that, near the critical point, the behavior of the diameter $\Delta\rho_d$ is characterized by the scaling term $t^{1-\alpha}$

$$\Delta\rho_d = 1 + B_2 t^{1-\alpha} - B_3 t \quad (4)$$

where $\Delta\rho_d = (\rho^+ - \rho^-)/2\rho_c$ and ρ^+ and ρ^- are the liquid and vapor saturated densities, differing from those of Fisher and Orkoulas,⁴⁰ who showed that the Yang–Yang anomaly implies a leading correction term $t^{2\beta}$ dominating the previously expected correction term $t^{1-\alpha}$.⁴⁶ Figure 10 compares $\Delta\rho_d$ calculated from eq 4 to that from an equation reported by Simon²⁰ together with the present measurements. Figure 10 shows that the Simon equation cannot be used to describe singular-diameter behavior.

For coexisting phases the relation of Yang and Yang⁴⁷ is

$$\frac{C_{V2}}{T} = -\frac{d^2\mu}{dT^2} + V\frac{d^2P_S}{dT^2} \quad (5)$$

**Figure 11.** Two-phase isochoric heat capacities of toluene as a function of specific volume along various isotherms: ●, measured two-phase isochoric heat capacity; ○, measured two-phase isochoric heat capacity at saturation.

where C_{V2} is the two-phase isochoric heat capacity, V is the specific volume, μ is the chemical potential, and P_S is the vapor pressure. According to eq 5, the two-phase isochoric heat capacity C_{V2} is a linear function of the specific volume V along each fixed isotherm (see Figure 11), the slopes of which equal $T(d^2P_S/dT^2)$, while the intercepts for $V=0$ are equal to $-T(d^2\mu/dT^2)$. The rapidly increasing slopes of the isotherms in Figure 11 as the critical temperature is approached reflect an increase of the second temperature derivative d^2P_S/dT^2 . From eq 5, it follows that the saturated heat capacities of liquid (C_{V2}) and vapor (C'_{V2}) in the two-phase states are related to the second temperature derivatives (d^2P_S/dT^2) and ($d^2\mu/dT^2$) by

$$\frac{d^2P_S}{dT^2} = \frac{C'_{V2} - C_{V2}}{T(V' - V)} \quad \text{and} \quad \frac{d^2\mu}{dT^2} = \frac{V'C_{V2} - VC'_{V2}}{T(V - V')} \quad (6)$$

where V' and V are the specific volumes of vapor and liquid at saturation, respectively, corresponding to a given temperature T . The measured two-phase liquid and vapor isochoric heat capacity data at saturation (C_{V2} , C'_{V2}) for toluene were used to derive a set of second derivatives d^2P_S/dT^2 and $d^2\mu/dT^2$ from eq 6. The results are given in Table 5. These data are useful to establish and test the quality of a vapor pressure equation $P_S(T)$ (see Figure 12). The derived second temperature derivatives d^2P_S/dT^2 for toluene have been described by using the scaling relation

$$\frac{d^2P_S}{dT^2} = P_1 t^{-\alpha} + P_2 t^{-\alpha+\Delta} + P_3 \quad (7)$$

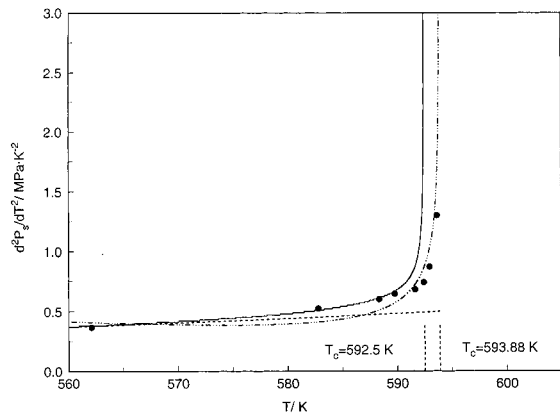
where the fitting parameters P_i are $P_1 = 2.0650 \pm 0.111$, $P_2 = 3.3647 \pm 0.327$, and $P_3 = -3.4774 \pm 0.243$ ($\chi^2 = 1.46$).

The vapor pressure equation derived from isochoric heat capacity measurements is

$$P_S(T) = P_c + \left(\frac{dP_S}{dT}\right)_c (T - T_c) + \Delta P_S(T) \quad (8)$$

Table 5. Second Temperature Derivatives (d^2P_S/dT^2) and ($d^2\mu/dT^2$) from Measured Two-Phase Isochoric Heat Capacities of Toluene

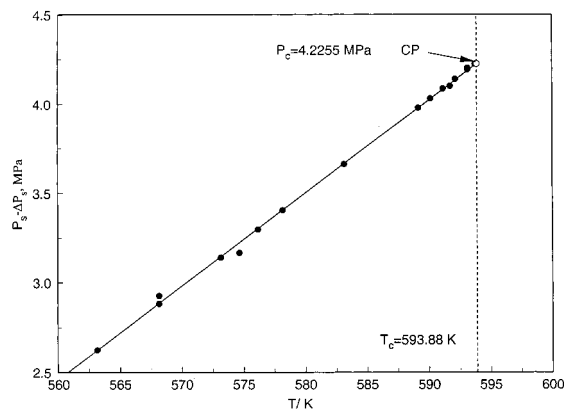
| T_S K | (d^2P_S/dT^2) kPa·K ⁻² | $(d^2\mu/dT^2)$ J·kg ⁻¹ ·K ⁻² |
|------------|--|--|
| 562.12 | 0.366 | -5.227 |
| 582.78 | 0.523 | -5.434 |
| 588.35 | 0.599 | -5.570 |
| 589.77 | 0.644 | -5.620 |
| 591.63 | 0.681 | -5.777 |
| 592.42 | 0.740 | -5.770 |
| 592.96 | 0.870 | -5.596 |
| 593.65 | 1.300 | -4.875 |
| 593.85 | 4.927 | 5.695 |
| 593.86 | 6.025 | 8.975 |

**Figure 12.** Second temperature derivatives d^2P_S/dT^2 derived from liquid and vapor two-phase isochoric heat capacity measurements along the coexistence curve for toluene together with values calculated from vapor pressure equations: ●, this work from C_V measurements; (---) Mamedov and Akhundov;¹² (—) Chirico et al.¹⁵; (····) from eq 8.

where $(dP_S/dT)_c$ is the value of the first temperature derivative of the vapor pressure at the critical point, P_c is the critical pressure, and $\Delta P_S(T) = \int_{T_c}^T dT \int_{T_c}^T (C'_{V2} - C_{V2})/[T(V' - V)] dT$ is the curvature of the vapor pressure curve, which can be calculated from $(C'_{V2}, C_{V2}, V', V, T)$ measurements at saturation. The values of $\Delta P_S(T)$ have been calculated by means of eq 7. Using selected vapor pressure ($P_S - T_S$) data recommended by Goodwin⁸ far from the critical point, and the present $(C'_{V2}, C_{V2}, V', V, T)$ measurements on the coexistence curve, one can estimate from eq 8 the values of the critical pressure P_c and the slope of the vapor pressure curve $(dP_S/dT)_c$ at the critical point as the intercept and slope of the experimental $P_S^{\text{exp}}(T) - \Delta P_S(T)$ versus T curve, respectively (see Figure 13). The linearity of the experimental behavior of the $P_S^{\text{exp}}(T) - \Delta P_S(T)$ curve can be used as a criterion of consistency of the independent thermal ($P_S - T_S$) and calorimetric (C_VVT) measurements at saturation. Equation 8 has been used to estimate the critical pressure P_c and also the first temperature derivative of vapor pressure at the critical point $(dP_S/dT)_c$ for toluene. The results are $P_c = 4.225 \pm 0.008$ MPa and $(dP_S/dT)_c = 0.0521 \pm 0.004$ MPa·K⁻¹. These values agree with the values derived from PVT measurements from ref 48, $P_c = 4.2358$ MPa and $(dP_S/dT)_c = 0.05228$ MPa·K⁻¹.

Conclusions

New measurements of the isochoric heat capacity of toluene near the critical point are presented with an uncertainty of 2 to 3%. Measurements cover a range of

**Figure 13.** Linear part of the vapor pressure equation, eq 9: ●, from present C_{V2} and selected $P_S - T_S$ measurements.⁸ The solid line represents calculated values of the linear part of the vapor pressure curve $P_c + (dP_S/dT)_c(T - T_c)$.

temperatures from 411 to 620 K and densities from 199.3 to 525.0 kg·m⁻³, including the single- and two-phase regions and the coexistence curve. The saturated densities and temperatures derived from calorimetric experiments agree very well with literature data. Density deviations are about 2% in the critical region and 0.3% in the range far from the critical point. New critical parameters (critical temperature $T_c = 593.88 \pm 0.02$ K; critical densities, from coexisting densities, $\rho_c = 296.9 \pm 5$ kg·m⁻³ and, from extrapolation of C_V^{-1} to zero, $\rho_c = 293.8 \pm 5$ kg·m⁻³; and critical pressure $P_c = 4.225 \pm 0.008$ MPa) for toluene are derived from the measured values of saturated densities and heat capacities in the immediate vicinity of the critical point. Though the two results for the critical density from this work are within their uncertainty, we will refrain from making a recommendation for ρ_c . A soon-to-be-published study of multiple properties (pressure–volume–temperature, heat capacity jumps, etc.) by Kiselev⁴⁹ suggests that the best critical density is about $\rho_c = 294.4 \pm 2.5$ kg·m⁻³, which falls between our two results. This work contributes toward a future standard-reference formulation of the thermodynamic properties of toluene³⁰ and can be used to improve and develop a new fundamental EOS for toluene as a standard fluid. Further heat capacity measurements are necessary in the vapor and liquid regions far from the critical point to complete the database for developing a standard-reference formulation.

Acknowledgment

One of us (I.M.A.) thanks the Physical and Chemical Properties Division at the National Institute of Standards and Technology for the opportunity to work as a Guest Researcher at NIST during the course of this research.

Literature Cited

- (1) Nieto de Castro, C. A.; Li, S. F. Y.; Nagashima, A.; Trengove, R. D.; Wakeham, W. A. Standard reference data for the thermal conductivity of liquids. *J. Phys. Chem. Ref. Data* **1986**, *15*, 1073–1086.
- (2) Polikhronidi, N. G.; Abdulagatov, I. M.; Magee, J. W.; Stepanov, G. V. Isochoric heat capacity measurements for light and heavy water near the critical point. *Int. J. Thermophys.* **2001**, *22*, 189–200.
- (3) Polikhronidi, N. G.; Batyrova, R. G.; Abdulagatov, I. M. Isochoric heat capacity measurements of nitrogen tetroxide system at temperatures between 410 and 484 K and pressures up to 35 MPa. *Fluid Phase Equilib.* **2000**, *175*, 153–174.
- (4) Polikhronidi, N. G.; Batyrova, R. G.; Abdulagatov, I. M. Two-phase isochoric heat capacity measurements for nitrogen tetroxide in the critical region and Yang-Yang relation. *Int. J. Thermophys.* **2000**, *21*, 1073–1095.

- (5) Abdulagatov, I. M.; Polikhronidi, N. G.; Batyrova, R. G. Measurements of the isochoric heat capacities C_V of carbon dioxide in the critical region. *J. Chem. Thermodyn.* **1994**, *26*, 1031–1045.
- (6) Abdulagatov, I. M.; Polikhronidi, N. G.; Batyrova, R. G. Isochoric heat capacity and liquid–gas coexistence curve of carbon dioxide in the region of the immediate vicinity of the critical point. *Ber. Bunsen-Ges. Phys. Chem.* **1994**, *98*, 1068–1072.
- (7) Vargaftik, N. B. *Handbook of Physical Properties of Liquids and Gases*, 2nd ed.; Hemisphere: New York, 1983.
- (8) Goodwin, R. D. Toluene thermophysical properties from 178 to 800 K at pressures to 1000 bar. *J. Phys. Chem. Ref. Data* **1989**, *18*, 1565–1635.
- (9) Zotov, V. V.; Kireev, B. N.; Neruchev, Yu. A. Study of the equilibria properties of hydrocarbons on the coexistence curve using acoustic method. *Zh. Prikl. Mech. Tekh. Fiz.* **1975**, *2*, 162–164.
- (10) Okhotin, V. S.; Razumeichenko, L. A.; Kas'yanov, Yu. I. Equation of state and thermodynamic properties of liquid toluene derived from acoustic data. *Thermophysical Properties of Substances and Materials*; GSSSD: Moscow, 1991; Vol. 30, pp 20–33.
- (11) Lemmon, E. W.; Jacobsen, R. T. National Institute of Standards and Technology, Boulder, CO, personal communication, 1997.
- (12) Mamedov, A. M.; Akhundov, T. S. *Thermodynamic Properties of Gases and Liquids. Aromatic Hydrocarbons*; GSSSD: Moscow, 1978.
- (13) Magee, J. W.; Bruno, T. J. Isochoric (p, ρ, T) measurements for liquid toluene from 180 K to 400 K at pressures to 35 MPa. *J. Chem. Eng. Data* **1996**, *41*, 900–905.
- (14) Francis, A. W. Pressure–temperature–liquid density relations of pure hydrocarbons. *Ind. Eng. Chem.* **1957**, *49*, 1779–1786.
- (15) Chirico, R. D.; Steele, W. V. Reconciliation of calorimetrically and spectroscopically derived thermodynamic properties at pressures greater than 0.1 MPa for benzene and methylbenzene: The importance of the third virial coefficient. *Ind. Eng. Chem. Res.* **1994**, *33*, 157–167.
- (16) Zotov, V. V.; Neruchev, Yu. A.; Mel'nikov, G. A. Thermophysical properties of liquid toluene on the coexistence curve. *Thermophysical Properties of Substances and Materials*; GSSSD: Moscow, 1991, Vol. 30, pp 16–20.
- (17) Hales, J. L.; Townsend, R. Liquid densities from 293 to 490 K of nine aromatic hydrocarbons. *J. Chem. Thermodyn.* **1972**, *4*, 763–772.
- (18) Shraiber, L. S.; Pechenyuk, N. G. The temperature dependency of density of some organic liquids. *Russ. J. Phys. Chem.* **1965**, *39*, 429–430.
- (19) Rudenko, A. P.; Sperkach, V. S.; Timoshenko, A. N.; Yagupol'skii, L. M. The elastic properties of trifluoromethylbenzene along the equilibrium curve. *Russ. J. Phys. Chem.* **1981**, *55*, 1054–1055.
- (20) Simon, M. Method and instruments used at bureau of physical and chemical standards. XV. Critical constants and rectilinear diameter of 10 hydrocarbons. *Bull. Soc. Chim. Belg.* **1957**, *66*, 375–387.
- (21) Riedel, L. Liquid density in the saturated state. Extension of the theorem of corresponding states. II. *Chem.-Ing. Technol.* **1954**, *26*, 259–268.
- (22) Ambrose, D. Vapor-pressure of some aromatic hydrocarbons. *J. Chem. Thermodyn.* **1987**, *19*, 1007–1008.
- (23) Ambrose, D.; Broderick, B. E.; Townsend, R. The vapor pressures above the normal boiling point and the critical pressures of some aromatic hydrocarbons. *J. Chem. Soc. A* **1967**, 633–641.
- (24) Ambrose, D. *Vapor-Liquid Critical Properties*; National Physical Laboratory Report Chem. 107; NPL: Teddington, England, 1980.
- (25) Ambrose, D.; Cox, J. D.; Townsend, R. The critical temperatures of forty organic compounds. *Trans. Faraday Soc.* **1960**, *56*, 1452–1459.
- (26) Tsionopoulos, C.; Ambrose, D. Vapor-liquid critical properties of elements and compounds. Aromatic compounds. *J. Chem. Eng. Data* **1995**, *40*, 547–558.
- (27) Powell, R. J.; Swinton, F. L. The thermodynamic properties of fluorocarbon + hydrocarbon mixtures. 3. Gas–liquid critical temperatures and comparison with the theory of Rowlinson and Sutton. *J. Chem. Thermodyn.* **1972**, *2*, 105–115.
- (28) Kobe, K. A.; Lynn, R. E. The critical properties of elements and compounds. *Chem. Rev.* **1953**, *52*, 117–236.
- (29) Marcos D. H.; Lindley, D. D.; Wilson, K. S.; Kay, W. B.; Hershey, H. C. A (p,V,T) study of tetramethylsilane, hexamethyldisiloxane, octamethyltrisiloxane, and toluene from 423 to 523 K in the vapor phase. *J. Chem. Thermodyn.* **1983**, *15*, 1003–1014.
- (30) Kudchadker, A. P.; Alani, G. H.; Zwolinski, B. J. The critical constants of organic substances. *Chem. Rev.* **1968**, *68*, 659–735.
- (31) Harand, J. The critical temperature as microchemical characteristic. *Monatsh. Chem.* **1935**, *65*, 153–184.
- (32) Fisher, R.; Reichel, T. Determination of the critical temperature with the micromelting-point apparatus. *Mikrochem. Acta* **1943**, *31*, 102–108.
- (33) Partington, E. J.; Rowlinson, J. S.; Weston, J. F. The gas–liquid critical temperatures of binary mixtures. *Trans. Faraday Soc.* **1960**, *56*, 479–485.
- (34) Teja, A. S.; Rosenthal, D. J. The critical pressures and temperatures of twelve substances using a low residence time flow apparatus. *AIChE Symp. Ser.* **1990**, *86*, 133–137.
- (35) Teja, A. S.; Anselme, M. J. The critical properties of thermal stable and unstable fluids. I. 1985 Results. *AIChE Symp. Ser.* **1990**, *86*, 115–121.
- (36) Altschul, M. On the critical properties of some organic compounds. *Z. Phys. Chem.* **1893**, *11*, 577–597.
- (37) Roof, J. G. Three-Phase critical point in hydrocarbon–water systems. *J. Chem. Eng. Data* **1970**, *15*, 301–303.
- (38) Wilson, L. C.; Wilding, W. V.; Wilson, H. L.; Wilson, G. M. Critical point measurements by a new flow method and a traditional static method. *J. Chem. Eng. Data* **1995**, *40*, 765–768.
- (39) Krase, N. W.; Goodman, J. B. Vapor pressure of toluene up to the critical temperature. *Ind. Eng. Chem.* **1930**, *22*, 13.
- (40) Fisher, M. E.; Orkoulas, G. The Yang-Yang anomaly in fluid criticality: Experimental and scaling theory. *J. Chem. Phys.* **2000**, *113*, 7530–7545.
- (41) Sengers, J. V.; Levelt-Sengers, J. M. H. Thermodynamic behavior of fluids near the critical point. *Annu. Rev. Phys. Chem.* **1986**, *37*, 189–222.
- (42) Chen, J.-H.; Fisher, M. E.; Nickel, B. J. Unbiased estimation of corrections to scaling by partial differential approximants. *Phys. Rev. Lett.* **1982**, *48*, 630–634.
- (43) Fisher, M. E.; Liu, A. J. The three-dimensional Ising model revisited numerically. *Physica A* **1989**, *156*, 35–76.
- (44) Bagnuls, C.; Bervilliev, C.; Meiron, D. I.; Nickel, B. C. Non-asymptotic critical behavior from field theory at $d = 3$. II. The ordered-phase case. *Phys. Rev. B* **1987**, *35*, 3585–3607.
- (45) Ley-Koo, M.; Green, M. S. Revised and extended scaling for coexisting densities of SF_6 . *Phys. Rev. A* **1977**, *16*, 2483–2491.
- (46) Mermin, N. D. Solvable model of a vapor-liquid transition with a singular coexistence-curve diameter. *Phys. Rev. Lett.* **1971**, *26*, 169–172.
- (47) Yang, C. N.; Yang, C. P. Critical point in liquid–gas transitions. *Phys. Rev. Lett.* **1969**, *13*, 303–305.
- (48) Akhundov, T. S.; Abdullaev, F. G. Specific volumes of toluene in the critical region. *Izv. Vys. Ucheb. Zaved. Neft Gas.* **1974**, *1*, 62–66.
- (49) Kiselev, S. B. Colorado School of Mines, Golden, CO, personal communication, 2001.

Received for review August 10, 2000. Accepted February 13, 2001. This work was supported by the Grant of RFBR 00-02-17856 and INTAS 96-1989.

JE000269Y